

Electronic Supporting Information

Phenyl-grafted carbon nitride semiconductor for photocatalytic CO₂-reduction and rapid degradation of organic dyes

Devthade Vidyasagar,^a Nilesh Manwar,^b Akanksha Gupta,^a Sachin G Ghugal,^c Suresh S Umare,^{a*} and Rabah Boukherroub^d

^a Materials and Catalysis Laboratory, Department of Chemistry, Visvesvaraya National Institute of Technology (VNIT), Nagpur, Maharashtra, 440010, India. Email: ssumare@chm.vnit.ac.in, ssumare1965@gmail.com, Fax: +91 712 2223230, Tel: +91 712 2801316.

^b Chemical and Material Science Division (CMSD), CSIR-Indian Institute of Petroleum (IIP), Mohkampur, Dehradun 248005, Uttarakhand, 248005, India.

^c School of Chemistry, Univ. of Hyderabad, Telangana, 500046, India.

^d Univ. Lille, CNRS, Centrale Lille, ISEN, Univ. Valenciennes, UMR 8520 – IEMN, F-59000 Lille, France.

Characterisation Details

The phase identification of samples was performed in the 2θ range between 10° and 80° using an X-ray diffractometer (Rigaku: Miniflex-II-DD34863) using Cu K α radiation ($\lambda = 0.15418$ nm) operated at 30 kV and 15 mA at a scan rate of 5° min^{-1} . The TEM images were recorded using a FEI Tecnai T-20 electron microscope operating at 300 kV. Energy dispersive X-ray spectroscopy analysis was carried out using Zeiss FESEM. UV-visible diffuse reflectance spectra (UV-Vis DRS) of all samples were recorded using a Jasco (model V-670) spectrophotometer equipped with an integrating sphere accessory. Barium sulfate was used as reference for the reflectance spectra. Fourier transform infrared (FT-IR) spectra were obtained on Shimadzu IRAffinity-1S spectrophotometer. The chemical composition and oxidation states of the materials were probed using ESCALAB 250-Xi X-ray photoelectron spectrometer microprobe. Surface area analysis was probed by Brunauer–Emmet–Teller (BET) method using a Micromeritics ASAP 2020 V3.04 H surface area analyzer by nitrogen adsorption at 77 K. Photoluminescence (PL) decays and PL lifetime images were recorded on a time-resolved Micro-Time 200 confocal fluorescence lifetime imaging microscopy (FLIM) setup (PicoQuant) equipped with an inverted microscope (Olympus IX 71). All the measurements were performed under ambient conditions, at room temperature, on a powder deposited cover-slip. Samples were excited by a 405 nm ps diode pulse laser with a stable repetition rate of 20 MHz (FWHM: 176 ps). The data acquisition was performed with a SymPhoTime software controlled PicoHarp 300 time-correlated single-photon counting (TCSPC) module in a time tagged time-resolved mode. The overall resolution of the setup was 4 ps.

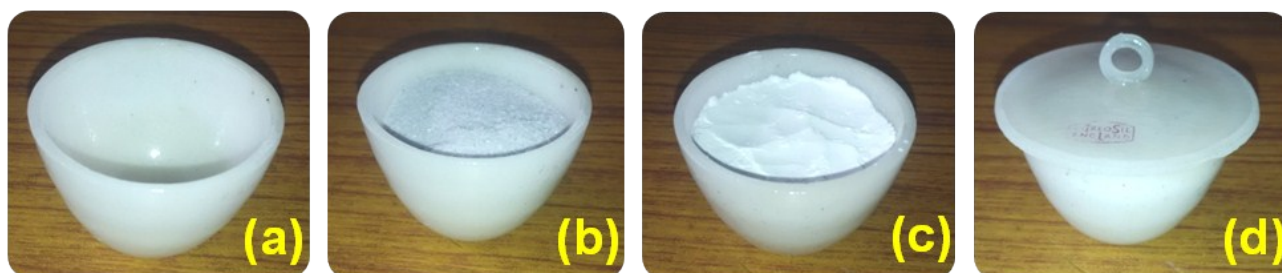


Figure S1. The stepwise procedure of phenyl grafted $g\text{-C}_3\text{N}_4$ synthesis: (a) empty silica crucible, (b) mixture containing 10 g of urea, 20 mg of phenyl urea, (c) protective covering using 1.5 g melamine, (d) final closing with silica lid to inhibit the escape of gases.

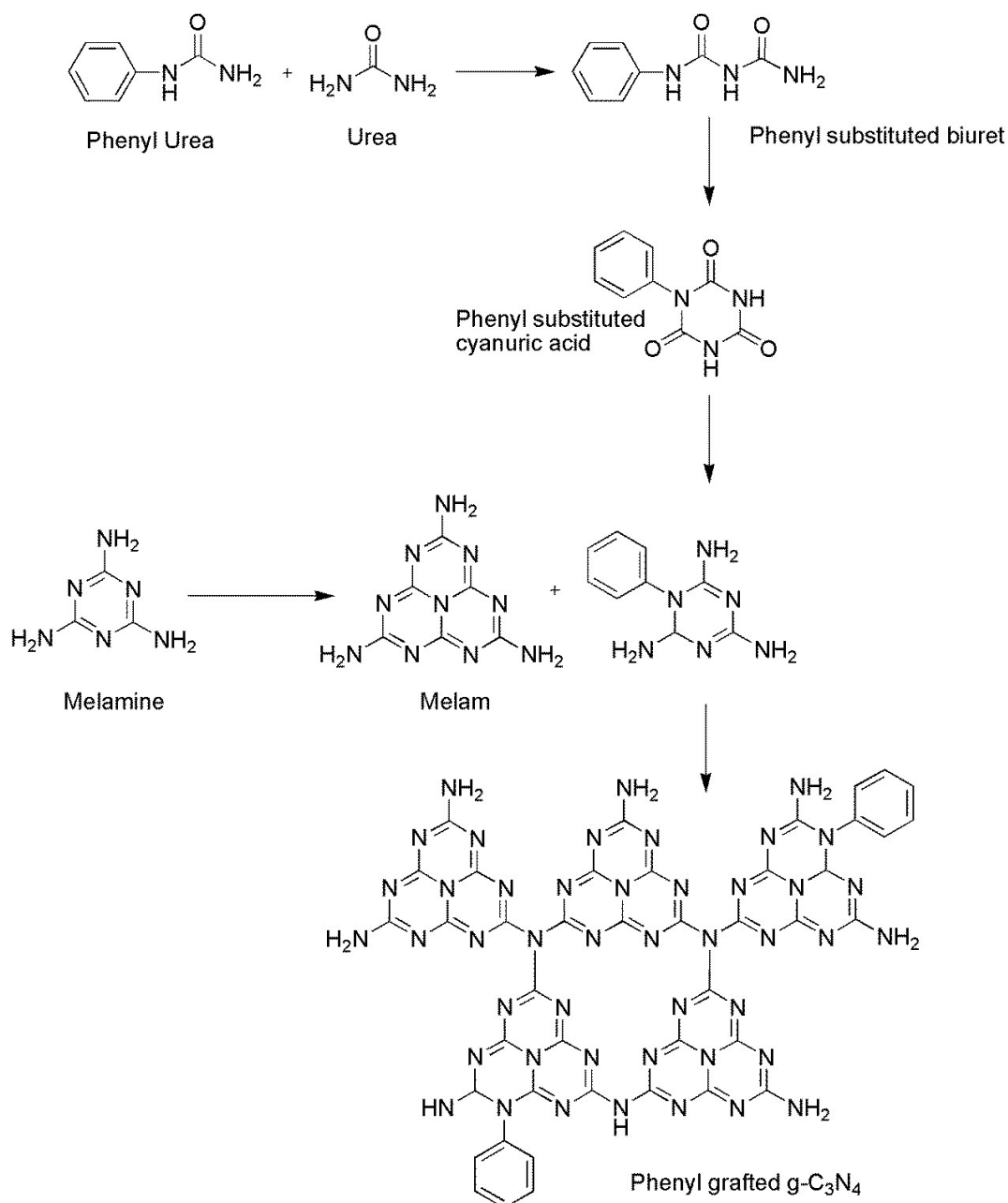


Figure S2. A plausible mechanism for the formation of Ph- $g\text{-C}_3\text{N}_4$ network obtained by thermal copolymerisation of phenyl urea, melamine and urea.

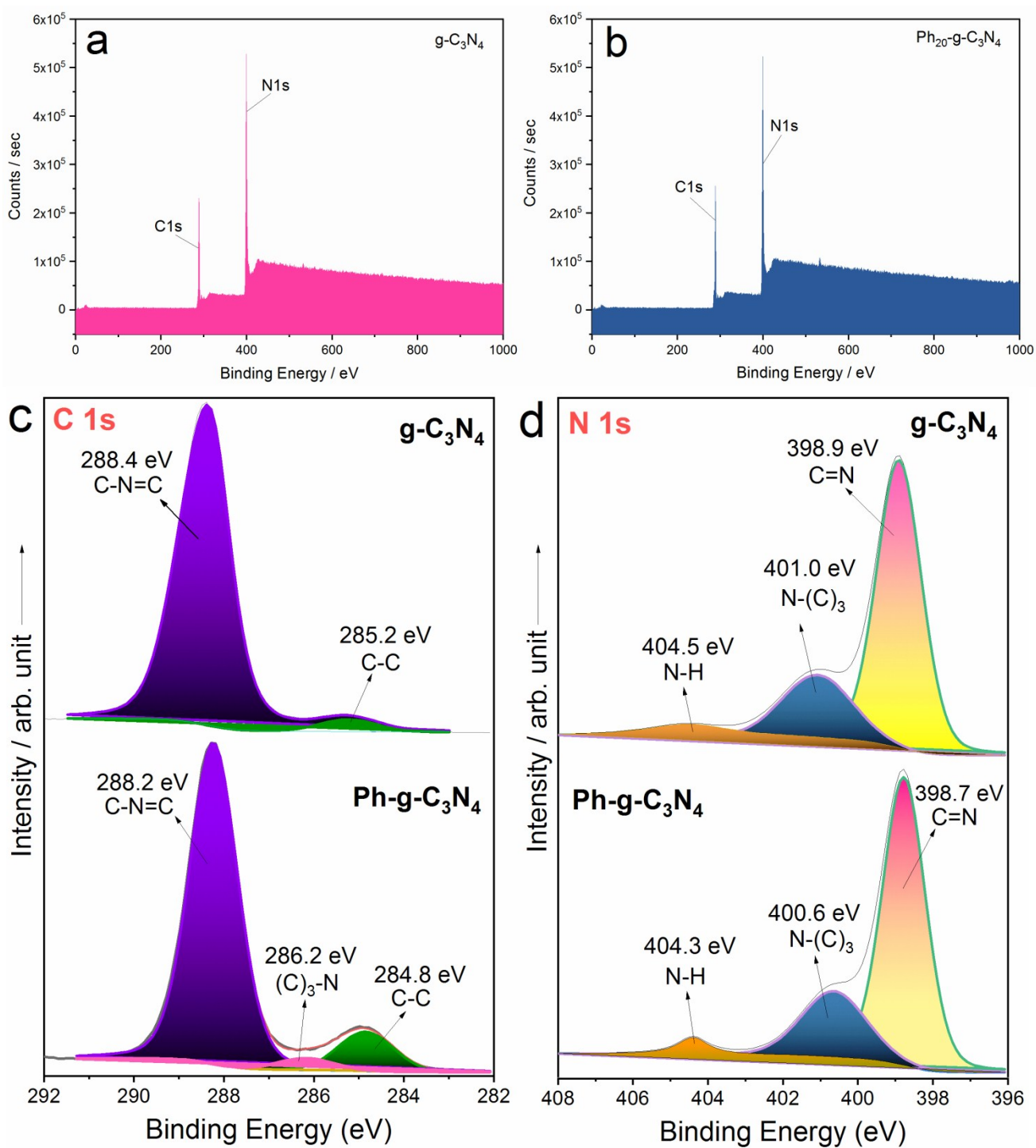


Figure S3. XPS survey spectra of (a) $g\text{-C}_3\text{N}_4$ (b) $\text{Ph-g-C}_3\text{N}_4$ and high-resolution XPS spectra of (c) C1s and (d) N1s of $g\text{-C}_3\text{N}_4$ and $\text{Ph}_{20}\text{-g-C}_3\text{N}_4$

Table S1. XPS peak parameters table.

Sample	Peak	Binding Energy	FWHM (eV)	Area (P) CPS. eV	Atomic (%)	C/N Ratio
$g\text{-C}_3\text{N}_4$	N 1s	399.23	2.62	1126736.26	54.81	0.77
	C 1s	288.33	1.44	563747.81	42.67	
$\text{Ph}_{20}\text{-g-C}_3\text{N}_4$	N 1s	399.15	2.62	1123842.10	52.7	0.84
	C 1s	288.21	2.32	612206.66	44.67	

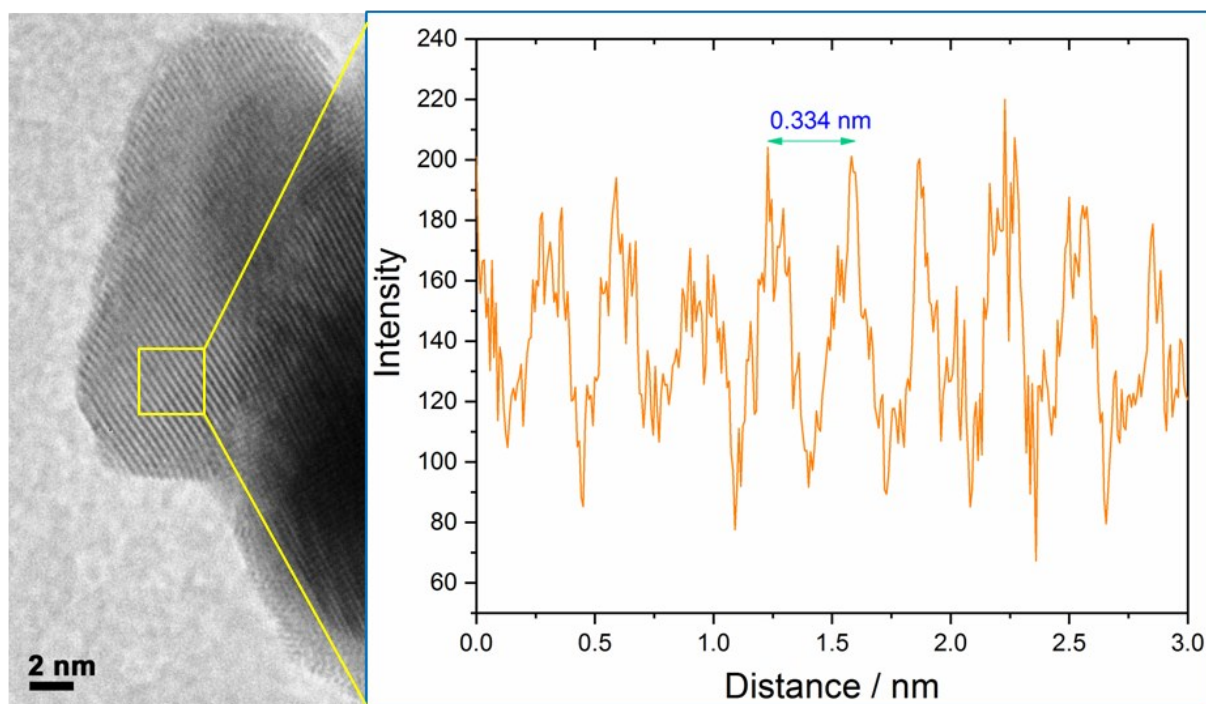


Figure S4. Plot profile graph of $\text{Ph}_{20}\text{-g-C}_3\text{N}_4$ HRTEM image selected portion obtained by ImageJ 1.50b software.

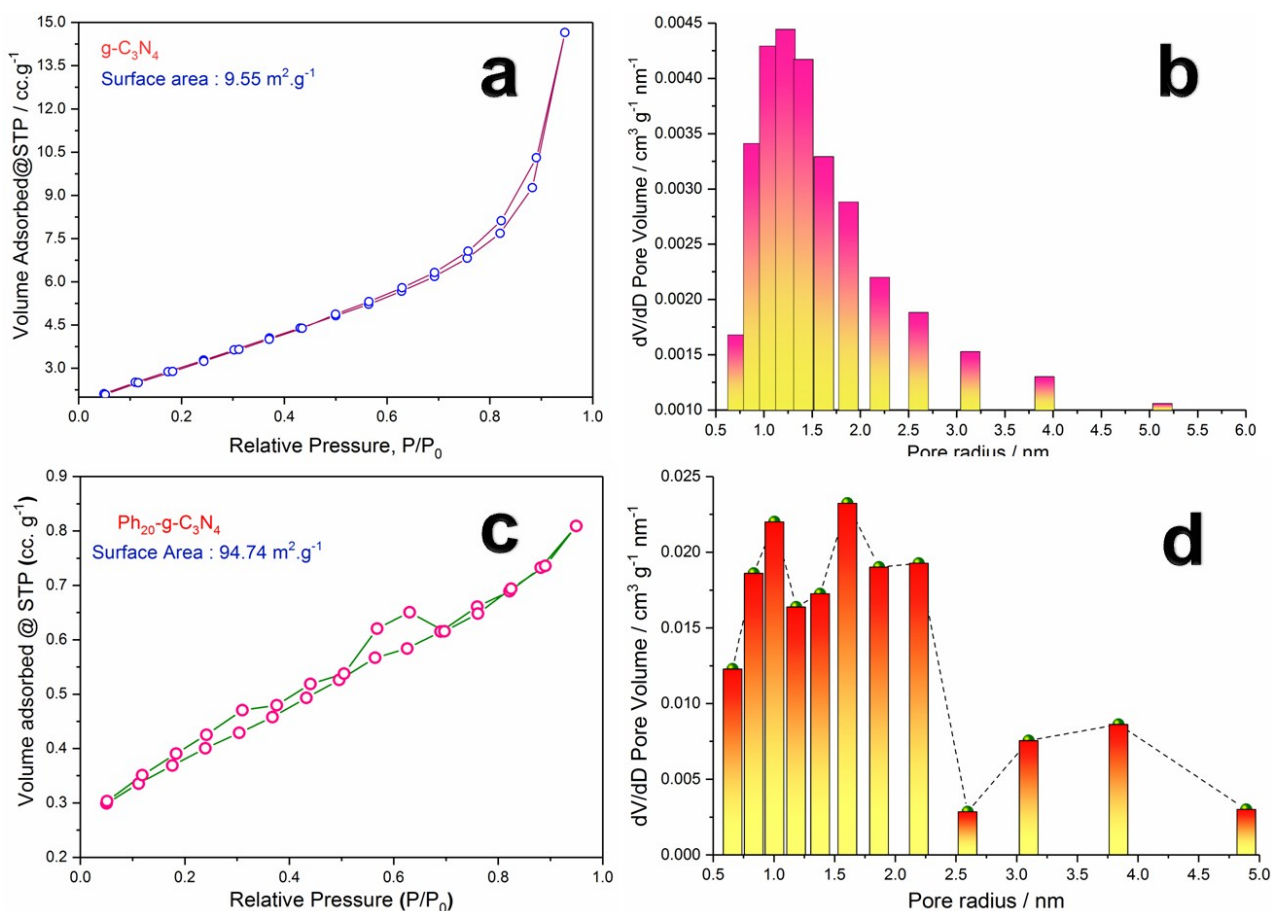


Figure S5. N_2 adsorption-desorption and pore-size distribution plots of (a, b) $\text{g-C}_3\text{N}_4$ and (c, d) $\text{Ph}_{20}\text{-g-C}_3\text{N}_4$, respectively.

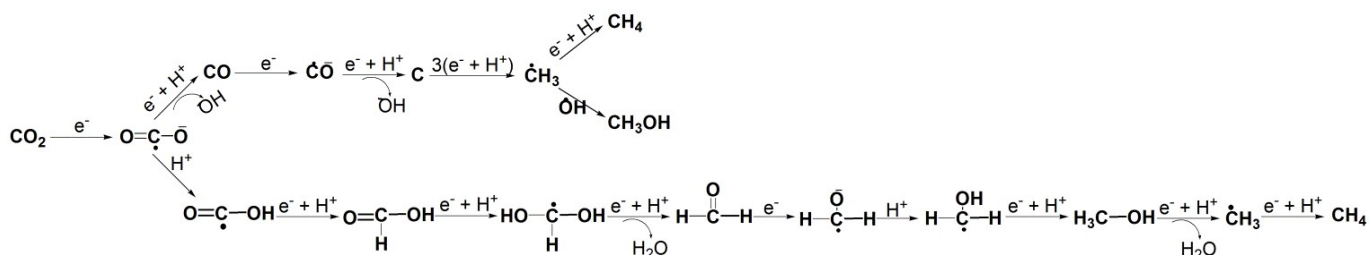


Figure S6. Plausible reactions pathway for CO₂ photoreduction into corresponding hydrocarbon products.

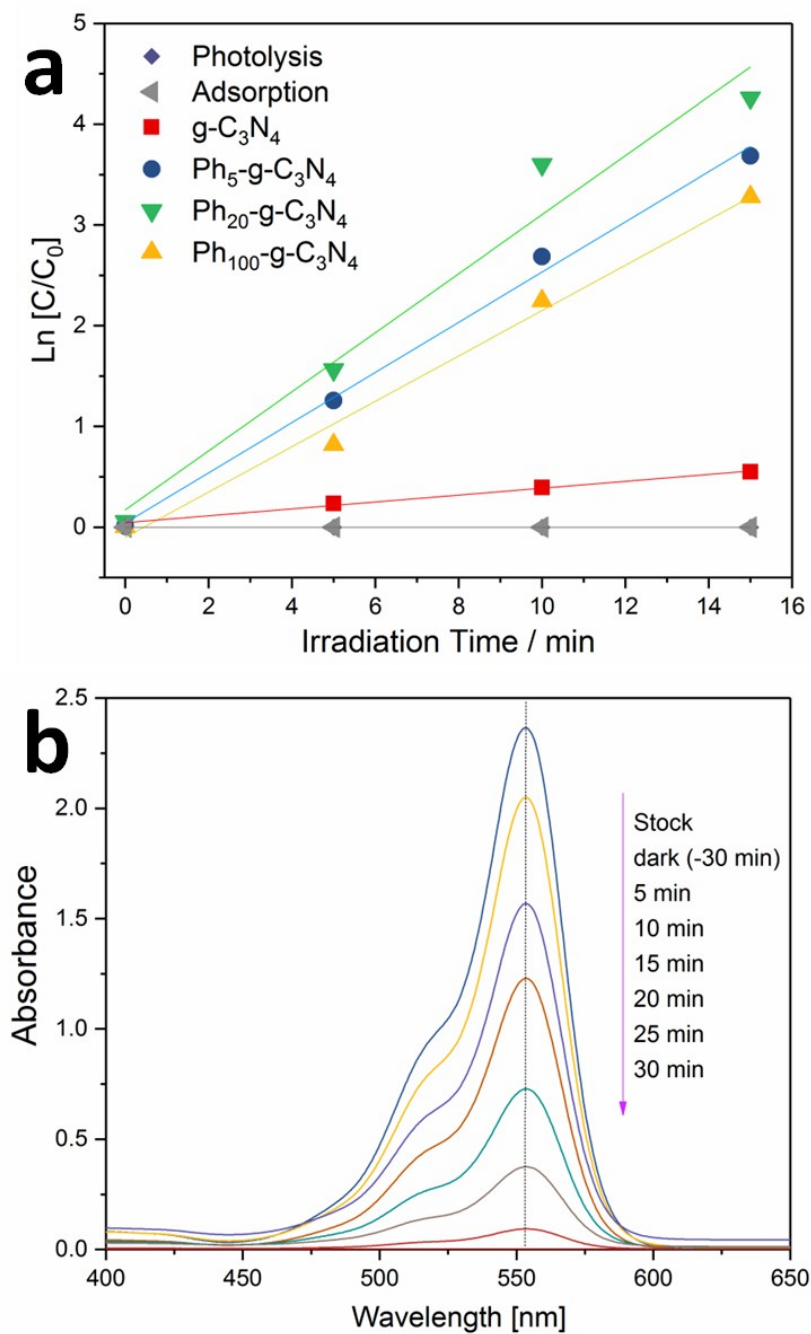


Figure S7. (a) Kinetic data of linear regression using various catalysts and (b) Temporal decay in UV-visible absorbance of RhB dye over Ph-g-C₃N₄ catalyst.

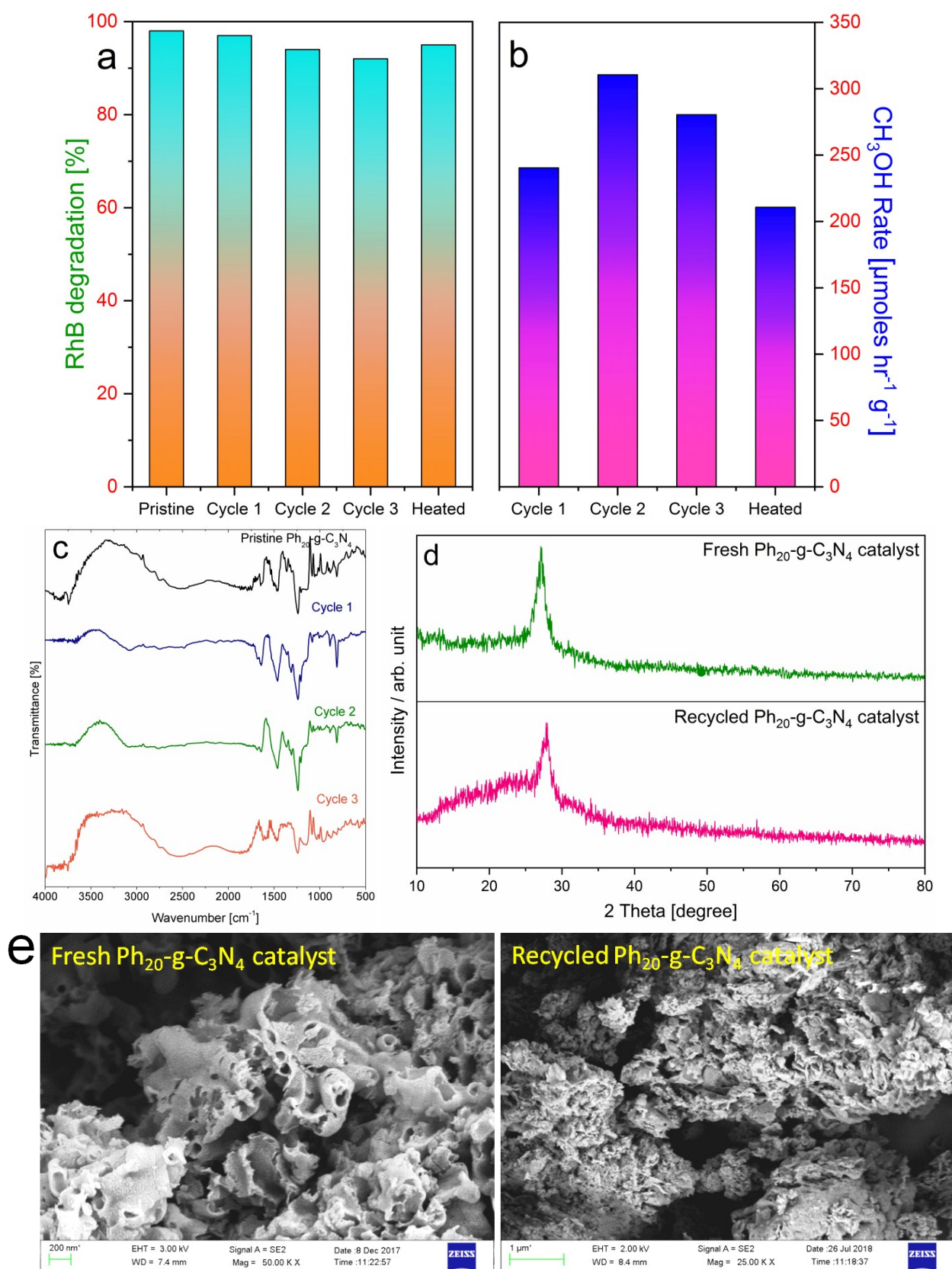


Figure S8. Recyclability test of (a) RhB degradation, (b) CH₃OH production using Ph₂₀-g-C₃N₄ catalyst, (c) FT-IR spectra of the corresponding catalyst after each cycle and (d, e) comparative XRD and SEM images of recycled catalyst after 3 cycles.

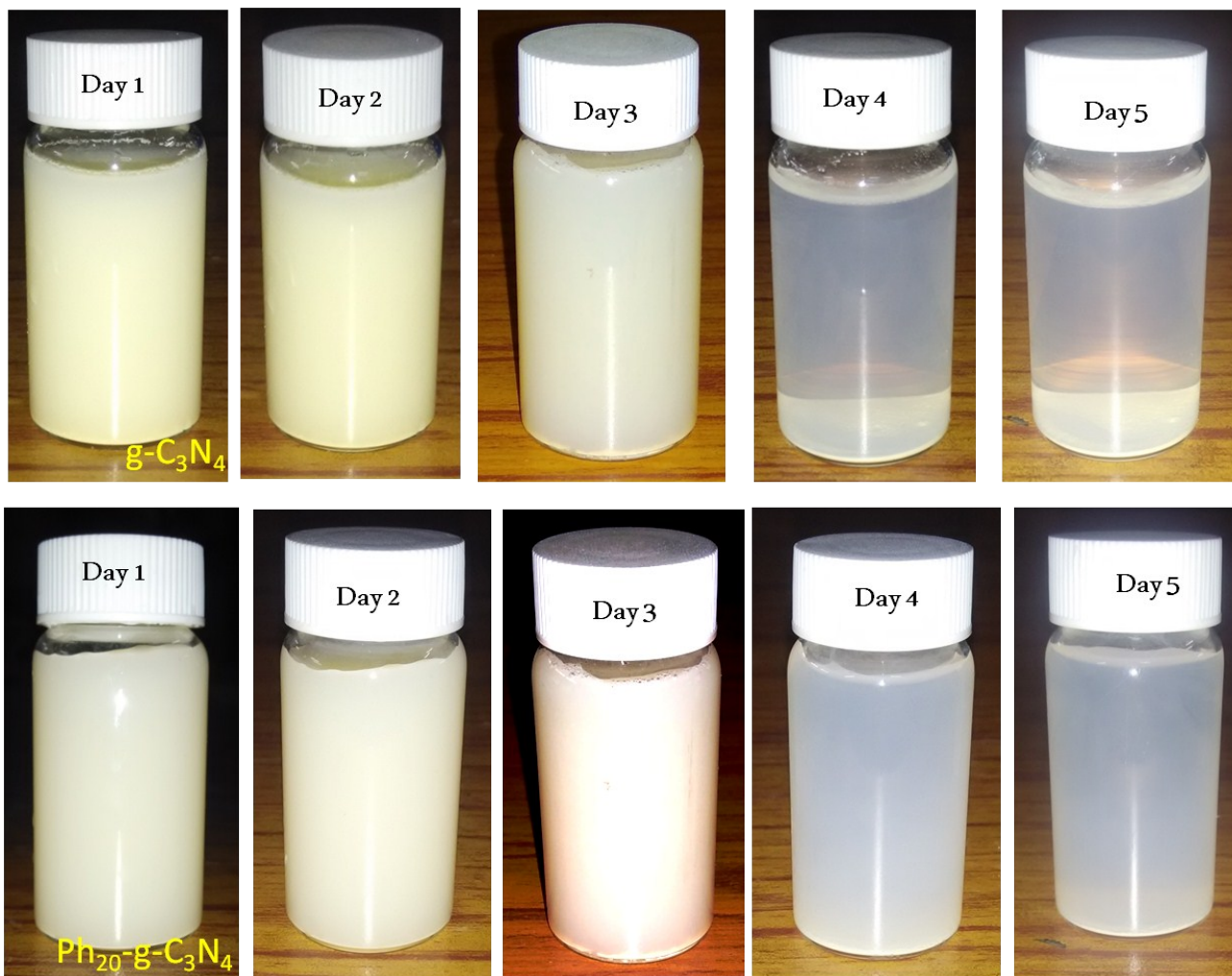


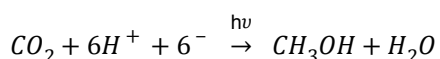
Figure S9. Dispersion properties of $g\text{-C}_3\text{N}_4$ (upper row) and $\text{Ph}_{20}\text{-g-C}_3\text{N}_4$ (second row) in water maintained at room temperature.

Table S2. Comparison of the $\text{Ph}_x\text{-g-C}_3\text{N}_4$ catalyst CO_2 photoreduction performance with reported photocatalysts.

Catalyst	Main Products	Amount of Products ($\mu\text{moles g}^{-1}$)	Ref
ZnO/g-C ₃ N ₄	CO, CH ₃ OH, CH ₄ , and CH ₃ CH ₂ OH	CO : 38.7 $\mu\text{moles g}^{-1}$ CH ₃ OH : 19.0 $\mu\text{moles g}^{-1}$ CH ₄ : 5.4 $\mu\text{moles g}^{-1}$ CH ₃ CH ₂ OH : 2.5 $\mu\text{moles g}^{-1}$	1
In ₂ O ₃ (10 wt%)-g-C ₃ N ₄	CH ₄	76.7 mg L ⁻¹	2
30AgBr/pC ₃ N ₄	CH ₄	10.92 mol g ⁻¹	3
SnO ₂ /B-P co-doped g-C ₃ N ₄	CH ₄	49 $\mu\text{mol g}^{-1}$	4
Ag ₃ PO ₄ /g-C ₃ N ₄	CO, CH ₃ OH, CH ₄ , and CH ₃ CH ₂ OH	57.5 $\mu\text{mol h}^{-1} \text{g}^{-1}$	5
g-C ₃ N ₄ nanosheets	CH ₄ CH ₃ CHO	0.5 μmol 0.4 μmol	6
g-C ₃ N ₄ /NaNbO ₃ nanowires	CH ₄	6.4 $\mu\text{mol h}^{-1} \text{g}^{-1}$	7
Ph_x-g-C₃N₄	CH₄ CH₃OH HCOOH	0.907 μmol 445.5 $\mu\text{mol h}^{-1} \text{g}^{-1}$ 5.1 V/V%	This work

Quantum Yield Calculation:

CO_2 photoreduction to methanol quantum efficiency was determined for the following possible reaction:



$$\text{Quantum Yield (QY)} = \frac{N_{\text{MeOH}} (6 \times \text{Number of mole of MeOH per unit time})}{N_p (\text{Number of incident photons per unit time})}$$

Here, '6' is the number of electrons required for CO_2 reduction into methanol (MeOH). The number of moles of MeOH per unit time was measured from obtained CH_3OH rate (445.5 $\mu\text{mol h}^{-1} \text{g}^{-1}$)

$$N_{\text{MeOH}} = (6 \times \text{CH}_3\text{OH rate in mole h}^{-1} / 3600) / N_A$$

Where N_A is the Avagadro number (6.023×10^{23}).

$$\begin{aligned} N_{\text{MeOH}} &= [(6 \times 0.000445) / 3600] / 6.023 \times 10^{23} \\ &= 4.467\text{E}+17 \end{aligned}$$

In the present CO₂ photoreduction experimental setup, the 20W LED bulb is located inside the reactor, therefore it is difficult to calculate the absorbed photons. It is further measured by the ratio of total energy reaching the reactor per second to the energy absorbed photons (E_λ).

$$N_p = \text{Bulb Wattage} \div E_\lambda (hC/\lambda_{\max})$$

Where, Bulb wattage= 20W = 20 Joule/ Second; h is the Plank's constant (6.626 X 10⁻³⁴J.s); C is the velocity of light (3 x 10⁸ m/s); λ_{max} is the wavelength of absorbed photons, it is obtained from average value of absorption band edge for Ph₂₀-g-C₃N₄.

$$N_p = [20 \div (6.626 * 10^{-34} \times 3 \times 10^8) / 461]$$

$$= 4.64E+19$$

$$QY (\%) = (N_{\text{MeOH}} / N_p) * 100$$

$$= 0.96 \%$$

References

1. He, Y.; Wang, Y.; Zhang, L.; Teng, B.; Fan, M. High-Efficiency Conversion of CO₂ to Fuel over ZnO/g-C₃N₄ Photocatalyst. *Appl. Catal. B* **2015**, *168*, 1-8.
2. Cao, S.-W.; Liu, X.-F.; Yuan, Y.-P.; Zhang, Z.-Y.; Liao, Y.-S.; Fang, J.; Loo, S. C. J.; Sum, T. C.; Xue, C. Solar-to-Fuels Conversion over In₂O₃/g-C₃N₄ Hybrid Photocatalysts. *Appl. Catal. B* **2014**, *147*, 940-946.
3. Ong, W.-J.; Putri, L. K.; Tan, L.-L.; Chai, S.-P.; Yong, S.-T. Heterostructured AgX/g-C₃N₄ (X= Cl and Br) Nanocomposites Via a Sonication-Assisted Deposition-Precipitation Approach: Emerging Role of Halide Ions in the Synergistic Photocatalytic Reduction of Carbon Dioxide. *Appl. Catal. B* **2016**, *180*, 530-543.
4. Raziq, F.; Qu, Y.; Humayun, M.; Zada, A.; Yu, H.; Jing, L. Synthesis of SnO₂/BP Co-doped g-C₃N₄ Nanocomposites as Efficient Cocatalyst-Free Visible-Light Photocatalysts for CO₂ Conversion and Pollutant Degradation. *Appl. Catal. B* **2017**, *201*, 486-494.
5. He, Y.; Zhang, L.; Teng, B.; Fan, M. New Application of Z-Scheme Ag₃PO₄/g-C₃N₄ Composite in Converting CO₂ to Fuel. *Environ. Sci. Technol.* **2014**, *49*, 649-656.
6. Niu, P.; Yang, Y.; Jimmy, C. Y.; Liu, G.; Cheng, H.-M. Switching the Selectivity of the Photoreduction Reaction of Carbon Dioxide by Controlling the Band Structure of a g-C₃N₄ Photocatalyst. *Chem. Commun.* **2014**, *50*, 10837-10840.
7. Shi, H.; Chen, G.; Zhang, C.; Zou, Z. Polymeric g-C₃N₄ Coupled with NaNbO₃ Nanowires toward Enhanced Photocatalytic Reduction of CO₂ into Renewable Fuel. *ACS Catal.* **2014**, *4*, 3637-3643.